Drivers of Extreme Rainfall During the Extratropical Transition of Hurricane Matthew (2016)

Scott W. Powell and Michael M. Bell, Colorado State University, Fort Collins, CO

1. Introduction

- Hurricane Matthew paralleled the southeastern U.S. coast on 7-9 October 2016. On 8 and 9 October, it dumped over 250 mm of rain--and up to over 400 mm locally--along a swath located in the coastal plain of South and North Carolina and Tidewater Virginia. The heaviest rain was focused along a surface front that developed to the north and west of Matthew's center as the cyclone underwent extratropical transition (ET).

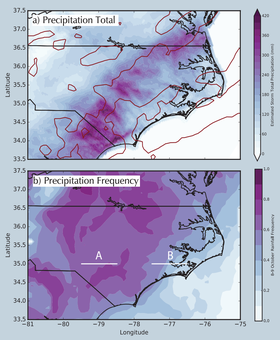

a) Total radar/rain gauge estimated rainfall during Matthew on 8-9 October. Frontogenesis = 1 K 3 hr^{-1} 100 km^{-1} outlined in red. b) Frequency of rainfall derived from radar. Cross sections referenced in Section 4.

- Some prior studies[1-3] have raised the possibility that cold air damming east of the Appalachian Mountains could enhance rainfall along the frontal boundary, presumably by making the cross-frontal temperature gradient larger.

- Release of conditional symmetric instability (CSI) as air rides isentropically over surface frontal boundary developed by the cyclone may also play an additional role in enhancing precipitation[4].

2. RAP Analyzed Synoptic Fields

500 hPa height (dm) and 250 hPa divergence

MSLP (hPa) and 2m Temperature (K)

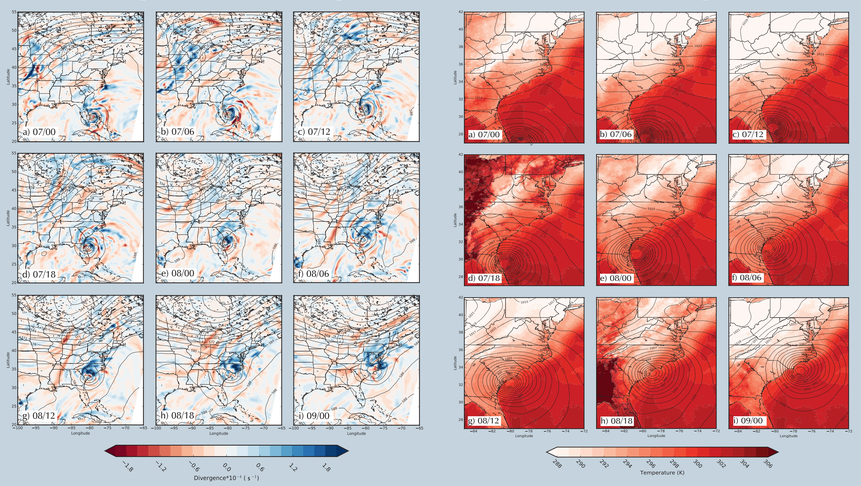

A negatively tilted trough approached Matthew from the northwest on 7-8 October, becoming positively tilted on 8 October, which is favorable for frontogenesis north of Matthew[2]. Divergence aloft spread north of the storm over eastern SC, NC, and VA.

High pressure over New England directed the pressure gradient southward along the coast, a favorable setup for cold air damming (CAD). Whether CAD definitely occurred is unclear above, but the surface front extending from Matthew is obvious by 08/12 UTC.

3. Numerical Model Experiments

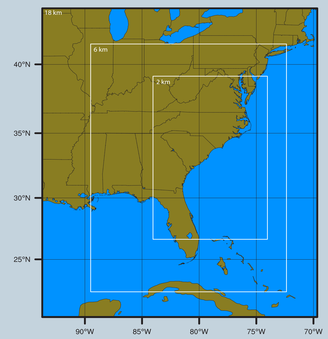

Domains used: 18-6-2 km, with no cumulus parameterization in inner domain.

Storm initialized almost entirely within inner domain at 07/06 UTC, a time early enough to allow CAD to develop during model integration rather than being imposed by initial conditions.

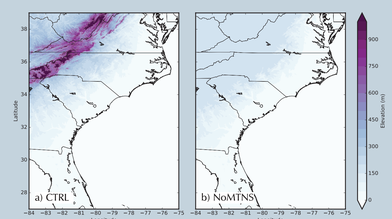

CTRL (control) experiment is compared to NoMTNS (no Appalachian mountains) experiment in which all terrain over 200m is flattened.

	Option
Boundary/Initial Conditions	ERA-Interim[5]/NOAA RTG SST
Microphysics	Thompson aerosol-aware[6]
Cumulus	Kain-Fristch[7] in 18/6 km
Land surface	Unified NOAH[8]
Radiation	RRTMG[9] longwave and shortwave
Planetary boundary layer	Yonsei University[10]

4. Simulated Rainfall with and Without Mountains

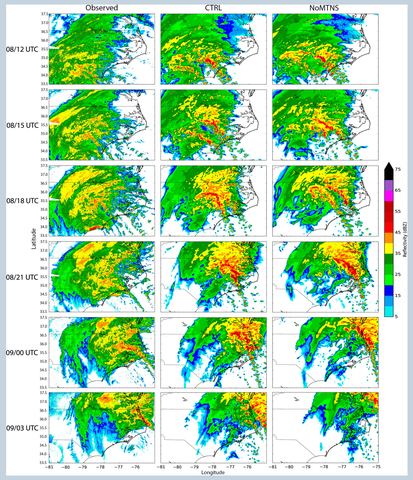

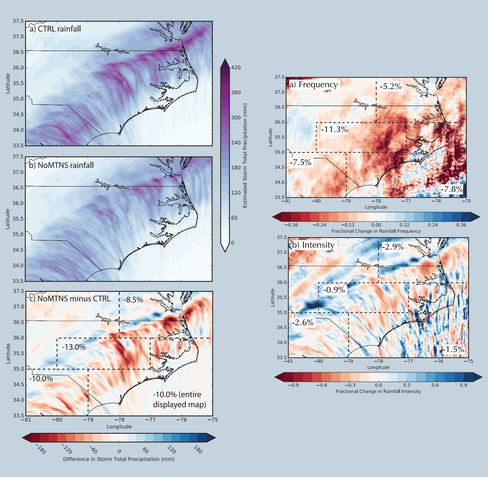

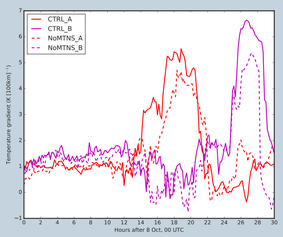

Top left) Observed WSR-88D reflectivity and simulated reflectivity in CTRL and NoMTNS runs from 30 to 45 hours after initialization.

Bottom left) Temperature gradient calculated across cross-sections A (red) and B (purple) in Section 1 for CTRL (solid) and NoMTNS (dashed) experiments.

Top center) Total rainfall on 8-9 October in CTRL and NoMTNS experiments. The difference in rainfall is plotted in the bottom panel, and percent changes in displayed subdomains are also shown.

Top right) Top panel illustrates change in rainfall frequency in NoMTNS simulation relative to CTRL run. Bottom panel shows the change in rainfall intensity.

5. Mesoscale Dynamics in the Rainbands

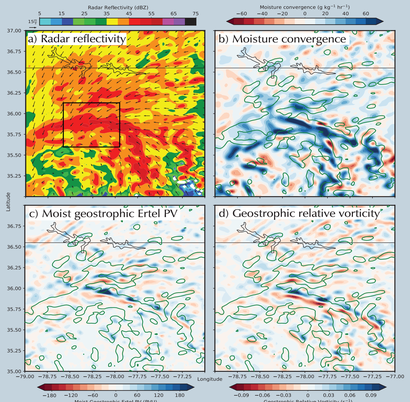

$$\wp_g = g\eta_g \cdot \nabla\theta_{es}$$

$$\wp_s = -g(\zeta_g + f)\frac{\partial\theta_e}{\partial p}$$

Moist geostrophic Ertel PV in panels (c).

$$\zeta_g = \frac{\partial u_g}{\partial x} + \frac{\partial v_g}{\partial y}$$

Geostrophic component of relative vorticity in panels (d).

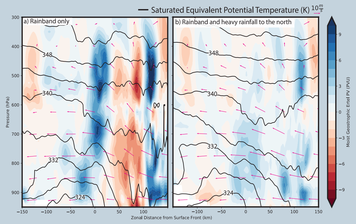

Top right) Cross sections of zonal/vertical wind (vectors), saturated equivalent potential temperature (black contours), and moist geostrophic Ertel PV (shading). Left panel is a cross section through rainband identified in top left at 18 UTC. Right panel is a cross section including rainband and heavy precipitation immediately to the north. CSI present ahead of surface front in rainband, but outside of narrow part of rainband CSI release is not responsible for intense rainfall.

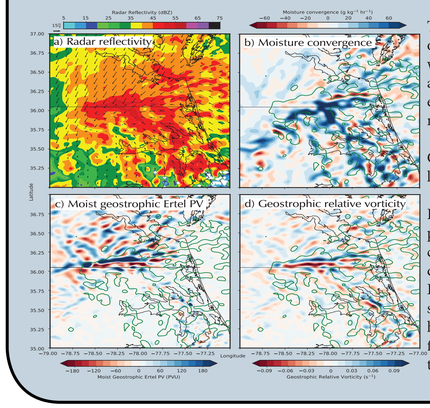

Top and bottom left) Two snapshots of simulated reflectivity (with 900 mb winds overlaid), and other variables at 900 mb. Top at 18 UTC over eastern NC; bottom 6 hours later over northeastern NC.

Green contours enclose 44 dBZ simulated reflectivity.

Low-level moisture convergence was present over most of the heavily precipitating area. Red in (c) panels indicates negative moist geostrophic Ertel PV--or areas where conditional symmetric instability was present. In heavily raining region, this was confined to a narrow strip in the center of the rainband.

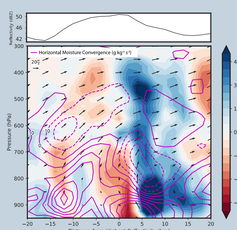

Bottom right) Mean meridional cross section through black box in top right figure. Vectors represent meridional and vertical wind. Purple contours denote moisture convergence. Strongest upward motion displaced from CSI maximum; however, reflectivity in rainband is greatest where CSI is present.

6. Conclusions

- Cold air damming has no obvious impact on the intensity of rainfall along a frontal boundary that developed across eastern NC during the ET of Matthew. Rainfall totals in a simulation with Appalachian Mountains are reduced by about 10% but only because the storm moves 10-15 % faster in that experiment. Intensity of rainfall in that experiment is reduced by less than 3%.

- Most of the simulated rainfall over NC during Matthew occurred within the narrow rainband. Extemely intense low-level moisture convergence (locally in excess of 50 g kg^{-1} hr^{-1}) was likely a primary driver for the rainfall.

- In a very small portion of the rainband (about 6 km across), conditional symmetric instability could have been released as air flowed upward over a surface frontal boundary developed by Matthew as it experienced ET; however, strongest vertical motions in rainband were displaced to north of CSI by <5 km.

S. Powell was supported by a NOAA Climate and Global Change Postdoctoral Fellowship, sponsored by UCAR's Cooperative Programs for the Advancement of Earth System Science. M. Bell acknowledges support from NSF grant AGS-1701225.

[1]Atallah and Bosart (2003), *MWR*, 1063-1081. [2]Atallah et al. (2007), *MWR*, 2185-2206. [3]Croke (2005), *M.S. Thesis, NCSU* [4]Colle (2003), *MWR*, 2905-2926. [5]Dee et al. (2011), *QJRMS*, 553-597. [6]Thompson and Eidhammer (2014), *JAS*, 3636-3658. [7]Kain (2004), *JAM*, 170-181. [8]Tewari et al (2004), *20th conf. on weather analysis forecasting/16th conf. on NWP* [9]Iacono et al. (2008), *JGR*, D13103. [10]Hong et al. (2006), *MWR*, 2318-2341.